Bulletin of the Seismological Society of America, Vol. 97, No. 4, pp. 1245–1258, August 2007, doi: 10.1785/0120060184

Aftershocks of the 1999 Chi-Chi, Taiwan, Earthquake: The First Hour

by Chien-Hsin Chang, Yih-Min Wu, Li Zhao, and Francis T. Wu

Abstract Within the hour immediately after the 1999 Chi-Chi mainshock, only 40 aftershocks were located by the Taiwan Central Weather Bureau Seismic Network (CWBSN) because of the power outage in more than half of the island and the limited dynamic range of the CWBSN high-gain instruments. Here, by analyzing 20 near-field, on-scale records from the Taiwan Strong-Motion Instrumentation Program (TSMIP), we determined a catalog of 296 aftershocks with $M_L \geq 3.4$ within the first hour after the Chi-Chi mainshock. Focal mechanisms were also determined for 24 of these aftershocks. The frequency-magnitude relation obtained from the 296 aftershocks indicates that the catalog is complete above magnitude M_L 4.3. Most of the aftershocks occurred in a small-slip region of the mainshock immediately to the north of the mainshock epicenter. Spatially, the aftershocks appear to migrate downward from the mainshock hypocenter. Later in the hour, the aftershocks began to concentrate in the fringe area of the main rupture. During the first hour, the *b*-value as defined by events in the $4.3 < M_L < 6$ magnitude range is about 1, the value of the background seismicity, and the frequency of larger events is higher.

Introduction

The Chi-Chi earthquake (M_w 7.6 and M_L 7.3) struck central Taiwan at 17:47 UTC, 20 September 1999 (1:47 a.m. local time on 21 September). As shown in the map in Figure 1, the surface break runs along the Chelungpu fault, a roughly 100-km-long north–south trending thrust fault dipping gently to the east with a maximum displacement more than 8 m (Chen *et al.*, 2001). The hypocenter was located at 23.853° N, 120.816° E with a depth of 8 km. The focal mechanisms determined by several groups consistently showed a thrust movement with strike, dip, and rake of about 5°, 34°, and 65°, respectively (Chang *et al.*, 2000).

Seismic networks in Taiwan, including the Central Weather Bureau Seismic Network (CWBSN), the Broadband Array in Taiwan for Seismology (BATS), and the Taiwan Strong-Motion Instrumentation Program network (TSMIP), have provided excellent spatial coverage in the Chi-Chi source region. The TSMIP records have already been used to study the slip history of the mainshock (e.g., Ma *et al.*, 2001; Ji *et al.*, 2003), and data from the other networks, the CWBSN in particular, were used to determine the spatial distribution and focal mechanisms of aftershocks (e.g., Kao and Chen 2000; Chen *et al.* 2002; Wu *et al.*, 2004). As is common with high-gain seismic networks, CWBSN records were clipped for most of the events immediately after the mainshock because of the limited dynamic range of the instruments. In addition, a large-scale electric power failure shut down most seismic stations in northern Taiwan (Wu *et al.*, 2000). As a result, only 31 CWBSN stations of a total of 71 (Fig. 1) provided records immediately following the Chi-Chi mainshock, and only 40 aftershocks could be located during the first hour after the occurrence of the mainshock. In contrast, the TSMIP strong-motion stations, used traditionally in engineering studies, successfully recorded on scale both the mainshock and many aftershocks immediately following the mainshock. Although in triggered mode, the TSMIP instruments were turned into continuous recording mode by the incessant $M_L > 3.5$ aftershocks in and around the source region, until the recording media were exhausted at the end of about one hour. Supplemented by the CWBSN data, these TSMIP records provided crucial data for a detailed investigation of the development of aftershock activity immediately following the mainshock. In this study, 20 TSMIP stations (Fig. 1) around the source region were selected to study the aftershocks within the hour following the Chi-Chi mainshock. We were able to identify and locate 296 events with magnitudes between 3.4 and 7.6. With the TSMIP data the completeness threshold for seismicity (Helmstetter *et al.*, 2005) is lowered significantly in the short period immediately after the mainshock, thus enabling us to trace the initial development and evolution of aftershocks in and around the source region.

TSMIP Records of Chi-Chi Earthquake and Its Aftershocks

The CWBSN consists of a central recording system in Taipei with 71 telemetered stations equipped with three-component S13 seismometers. It is the backbone system for

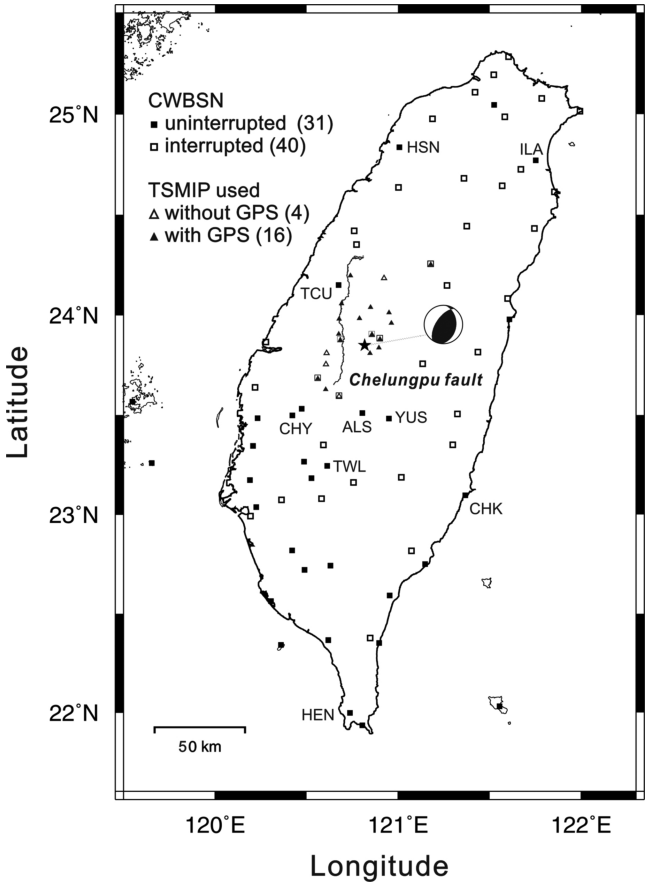

Figure 1. Map of Taiwan showing the epicenter of the Chi-Chi earthquake (star) and the locations of the CWBSN stations (squares). Filled and open squares indicate, respectively, the uninterrupted and interrupted stations immediately after the Chi-Chi mainshock. Triangles are the 20 TSMIP stations whose strong-motion records are used in this study. Open triangles indicate TSMIP stations without GPS timing system. The surface rupture of the Chelungpu fault and the focal mechanism of the Chi-Chi mainshock are also plotted.

ambient seismicity monitoring in and around the island of Taiwan. The seismic signals are digitized using 12 bits A/D at a rate of 100 samples per second. Even if the motion of the mass inside the S13 seismometer does not reach its mechanical stop, the CWBSN's 12-bit system in its high-gain operation mode can easily be saturated for events with magnitudes greater than about 4.0 at stations within 100 km from the epicenter.

On the other hand, the TSMIP stations are equipped with three-component, $\pm 2g$ full-scale force-balance accelerometers (FBA) with a 16-bit or higher resolution recorder and a sampling rate of 200 or 250 samples/sec. Nearly all TSMIP stations have recorded on scale all the large local earthquakes, although they also have a minimum magnitude cutoff. The TSMIP network consists of about 680 stations, out of which data from 20 stations were selected for this study (triangles in Fig. 1). The selection criteria for the stations are (1) the instruments are equipped with Global Positioning System (GPS) timing system (16 of the 20 used here), and (2) they provide good spatial coverage of the Chelungpu fault and the rupture zones. For the four stations without GPS systems (TCU137, TCU122, CHY024, and CHY080), we assign the predicted *P*-wave arrival time, calculated on the basis of a 3D velocity model (Wu *et al.*, 2006), to the actual *P*-wave onset of the mainshock at each station. At these four stations the *P*-wave onsets of the aftershocks are particularly clear and their inclusion enhances the station coverage.

Figure 2 displays the vertical-component strong-motion records for the first hour after the Chi-Chi mainshock at the 20 TSMIP stations along with the seismograms at 9 CWBSN stations close to the Chi-Chi epicenter. Locations of the selected TSMIP and CWBSN stations are shown in Figure 3. Except at three more distant stations (HSN, ILA, and HEN) the large-amplitude ground motions of the larger aftershocks saturated the high-gain 12-bit CWBSN recording systems within the one-hour time. In contrast, all 20 TSMIP records are on-scale. The clipping in the beginning of the TSMIP waveforms in Figure 2 is due to scaling factor in plotting them to render the later signals of smaller amplitudes visible. The excellent quality of the TSMIP records can also be seen in the magnified view of their waveforms in Figure 4. Unlike modern broadband instruments the TSMIP recording was triggered and the recorders were designed to hold a little over an hour of continuous data; our investigation of the Chi-Chi aftershocks cannot be extended to include the many larger aftershocks hours and days after the mainshock.

Determining Aftershock Locations and Focal Mechanisms

The hypocenter locations of the aftershocks were determined using both *P*- and *S*-wave arrival times taken from the TSMIP strong-motion and the available readings from nine CWBSN records. The 3D earthquake location method of Thurber and Eberhart-Phillips (1999) was used in this study. Theoretical travel times of *P* and *S* waves were calculated by raytracing (Thurber, 1993) in the regional 3D velocity model of Wu *et al.* (2006). Wu *et al.* (2006) combined a large dataset of *S*-*P* times from the TSMIP records with the *P*- and *S*-wave arrival times from the CWBSN network in imaging the regional 3D *P*-wave and V_p/V_s structures in Taiwan. The TSMIP dataset improves the source-station path coverage tremendously and provides much better constraints and resolution in velocity structure determination. In their results, after 3D location, the standard deviation of *P* and *S* travel-time residuals decreased by about 0.15 sec and 0.1 sec compared to those for the current CWB model, respectively. In particular, the standard deviation of the *S*-*P* residuals decreased by about 0.2 sec, a 42% drop.

During the first hour, an average of about five events occurred every minute and so it is not always straightforward to associate the arrivals with a particular event. Figure 4

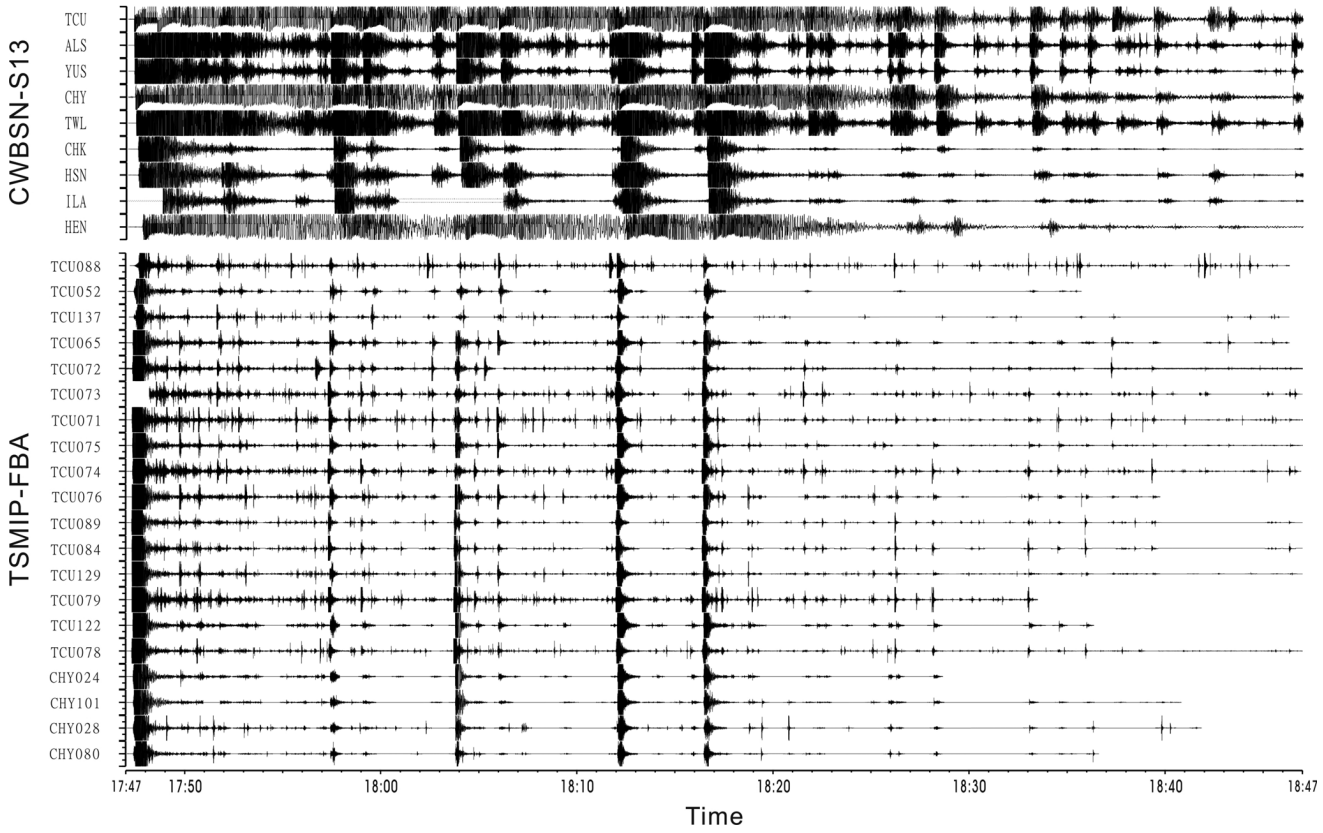

Figure 2. Seismograms recorded during the first hour after the Chi-Chi mainshock. The top nine traces are records from CWBSN stations near the epicenter. The bottom 20 traces are strong-motion records from TSMIP stations used in this study. Notice that the CWBSN records shown here clipped due to limited dynamic range, whereas all TSMIP records are on-scale.

shows two examples to illustrate our approach to event identification. A two-step procedure has been designed to pick the arrival times of *P* and *S* waves and to associate them with an event. For Event 110, for example, the four earliest and closely timed *P*-wave arrival times were first identified and picked from the vertical-component seismograms (Fig. 4, left column) at stations TCU079, TCU078, TCU084, and TCU089. These were used to determine a preliminary event location and origin time. This preliminary solution was then used to predict the *P*-wave arrival times at the other stations as well as *S*-wave arrival times at all stations using the 3D model of Wu *et al.* (2006). These predictions provide essential guidance for picking the *P*- and *S*-wave arrival times at as many stations as possible. For Event 110, a total of 37 *P*- and *S*-arrival times were used to determine its location and origin time. All the strong-motion records at the 20 selected TSMIP and CWBSN stations were analyzed following this procedure. In total, 296 aftershocks were located using the TSMIP records within 1 hour after the Chi-Chi mainshock. The events are listed in Table 1. For each event, at least six *P* or *S* arrivals were used. The root-mean-square (rms) value of the travel-time residuals was estimated to be 0.15 ± 0.08 sec. The uncertainties of the source depths (ERZ) and the epicentral locations (ERH) (Flinn, 1965) were estimated to be 0.5 ± 0.4 km and 0.5 ± 0.5 km, respectively.

In our determination of local magnitude M_L, the strong-motion records were first transformed to Wood–Anderson seismograms. For comparison and consistency with the CWBSN catalog, we used the attenuation relation of Shin (1993) in the magnitude calculation, instead of the one recently determined by Wu *et al.* (2005).

Using the polarities of the *P*-wave first motions, focal mechanisms of the aftershocks have also been investigated. As illustrated for Event 110 in Figure 3, the first-motion polarity observations of both the TSMIP and CWBSN stations were used to maximize the azimuthal coverage of the event. In total, focal mechanisms of 24 aftershocks within 1 hour of the Chi-Chi mainshock were determined and the results are summarized in Table 2.

Results and Discussion

Figure 5a shows the relation of magnitude versus origin time for the aftershocks within the 3.5 hours after the Chi-Chi mainshock. The 296 events determined in this study

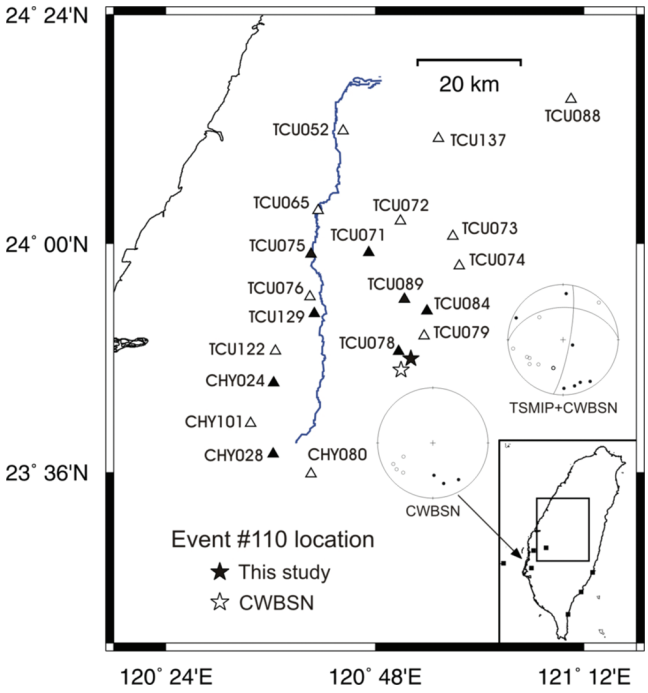

Figure 3. Regional map around the Chelungpu fault and the locations of the 20 TSMIP stations (triangles) selected for this study. Both CWBSN and our locations for Event 110 in Table 1 are indicated. The TSMIP stations we used to determine the location and focal mechanism of Event 110 are shown by filled triangles. Filled squares in the inset map show the seven CWBSN stations at which records are available for the determination of Event 110. The two focal spheres show that the mechanism of Event 110 cannot be determined with the seven CWBSN records alone, but a good solution can be derived by using both TSMIP and CWBSN records.

Figure 4. An example of accelerograms showing two closely timed aftershocks (Events 110 and 111; see Table 1 for event information) during the first hour after the Chi-Chi earthquake and our *P* and *S* picks. Plotted are the vertical (left panel) and east–west (right panel) components of the strong-motion accelerograms from the 20 TSMIP stations between 18:03:40 and 18:04:05, 20 September 1999. The vertical scales are given on top of each component. All the original records are on-scale and clipping for some of the traces results from the plotting scales chosen to display the details of the smaller-amplitude waves. The solid lines running continuously through all the traces indicate the origin times of the two events. The *P* arrivals are picked from the vertical records, whereas the *S* arrivals are picked from the horizontal components. For the examples shown here, the red and blue short solid lines on the vertical seismograms indicate the *P*-wave onset times of Events 110 and 111, respectively, whereas the same lines on the horizontal seismograms indicate the corresponding *S*-wave onset times. For Event 110, the earliest four *P*-wave arrival times (stations TCU079, TCU078, TCU084, and TCU089) were used to obtain a preliminary location of the event. The location was then used to calculate the arrival times of *P* waves at the other stations as well as *S* waves at all stations (red solid lines in the east–west component). These calculated arrival times were used to aid the identification and picking of the onset times of *P* and *S* waves. In total we were able to obtain arrival times of 37 phases for the final determination of the hypocentral location of Event 110. Event 111 and all the other events were located in the same way.

using the 20 TSMIP stations and those determined by the CWBSN are plotted with open and filled circles, respectively. Within the 33-minute time window between the time of the mainshock (shown as a star) and 18:20 UTC (dashed line), only 14 events were determined by using the CWBSN data, whereas a total of 210 aftershocks were identified and located by our interactive procedure using the TSMIP records. Figure 5b is the Gutenberg–Richter plot of the cumulative number of events N versus M_L for the 296 events. Our catalog appears to be complete above M_L 4.3. The straight-line portion of the curve (between $4.3 < M_L < 6.2$) yields a "normal" b-value of nearly 1 during the first hour, the value before the Chi-Chi earthquake (Wu and Chiao, 2006). There are evidently an abnormal number of larger ($M_L > 6$) events.

Figure 6a–c shows the distribution of hypocenters in mapview and in two vertical profiles within three time windows following the mainshock: from 0 to 5 minutes, from 5 to 15 minutes, and from 15 to 35 minutes, respectively. The hypocenters of all aftershocks within about 24 hours of the Chi-Chi mainshock located by all the networks are plotted in Figure 6d. The beachballs in Figure 6b–d are the 24 focal mechanisms determined in this study (Table 2). Most of the 296 aftershocks in the first hour have focal depths shallower than 20 km, although a few of them did reach a depth of about 30 km. All aftershocks have local magnitudes above 3.4, with more than 40 of them greater than magnitude 5.0. As shown in Figure 6a–c, all the aftershocks in the first hour can be used to define the Chelungpu fault. Also apparently, right after the mainshock, most of the aftershocks occurred north of the mainshock epicenter at depths ranging from 5 to 15 km, mostly deeper than the mainshock, although several aftershock studies (e.g., Wu *et al.*, 2004) have found that a noticeable number of $4 < M_L < 5$ events occurred to the north of the mainshock epicenter and above the main rupture surface.

During the first hour, it seems that aftershock activities didn't extend to the other structures such as the eastern Central Range (Wu *et al.*, 2004). However, within 24 hours seismic activities along the surrounding structures were well developed (Fig. 6d). All of the TSMIP stations used are located around the Chi-Chi earthquake rupture region, and thus the available data cannot resolve the seismicity elsewhere. From the constraints provided by the excellent coverage of our data in the Chi-Chi earthquake source rupture region, one thing is clear, during the first 15 minutes after the Chi-Chi mainshock most of the aftershocks occurred in an east-

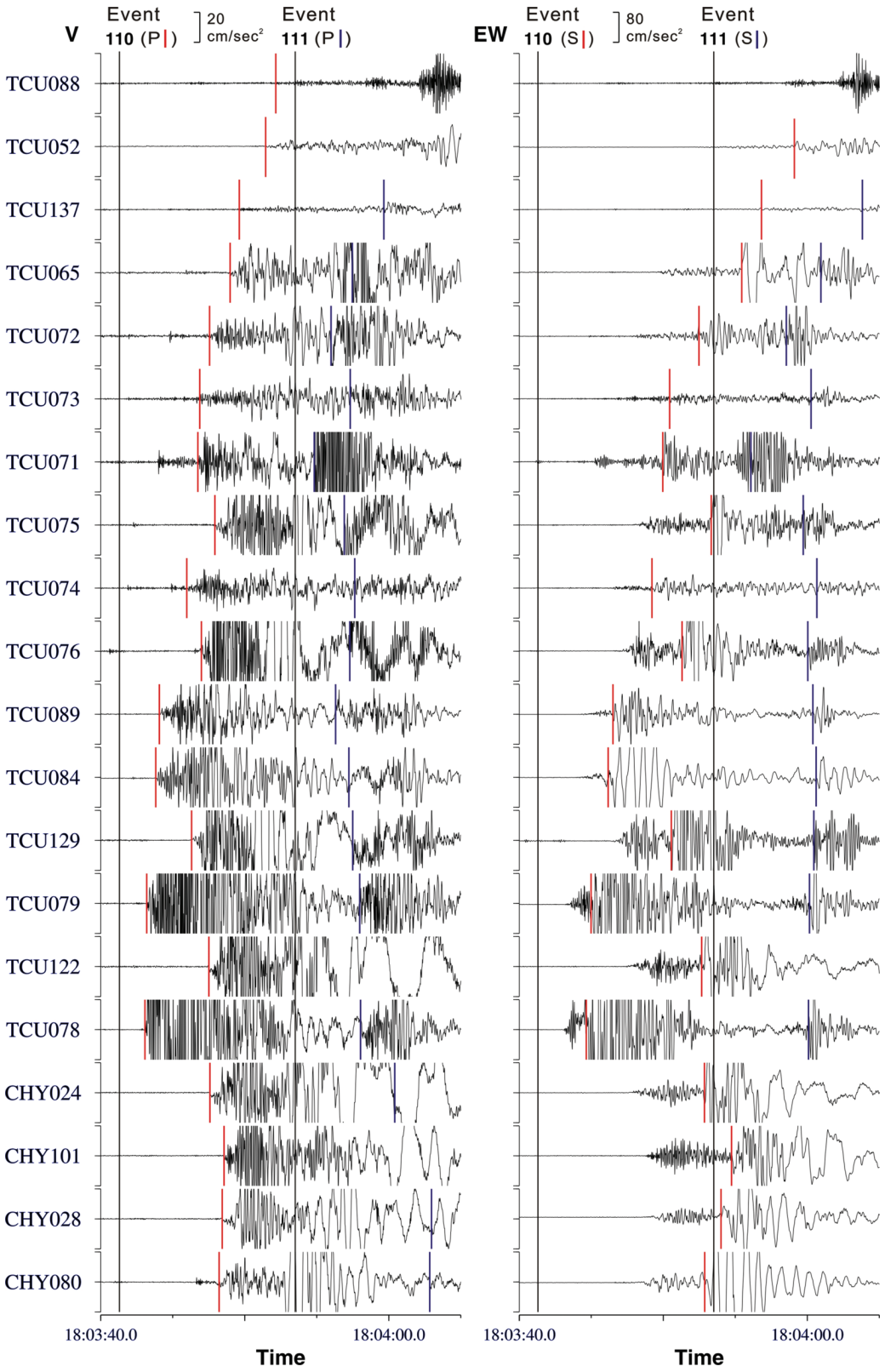
V
Event
110 (P|)
20
cm/sec²
Event
111 (P|)
EW
Event
110 (S|)
80
cm/sec²
Event
111 (S|)
TCU088
TCU052
TCU137
TCU065
TCU072
TCU073
TCU071
TCU075
TCU074
TCU076
TCU089
TCU084
TCU129
TCU079
TCU122
TCU078
CHY024
CHY101
CHY028
CHY080
18:03:40.0
18:04:00.0
Time
18:03:40.0
18:04:00.0
Time

Table 1
Parameters of the 296 Aftershocks Determined in This Study

No.	Origin Time (UT)	Latitude (° N)	Longitude (° E)	Depth (km)	M_L	RMS* (sec)	ERH† (km)	ERZ‡ (km)	No. Arrivals
1	1999/9/20 17:47:15.9	23.853	120.815	8.0	7.3	0.18	0.1	0.2	37
2	1999/9/20 17:48:04.2	24.051	120.940	8.9	5.6	0.17	0.5	0.6	10
3	1999/9/20 17:48:25.5	23.942	120.812	6.4	5.3	0.26	0.3	0.4	23
4	1999/9/20 17:48:26.3	23.898	120.920	10.3	5.1	0.04	0.3	0.1	8
5	1999/9/20 17:48:30.8	23.964	120.970	9.8	5.4	0.19	0.7	0.5	18
6	1999/9/20 17:48:40.0	23.962	120.974	10.6	5.2	0.27	1.2	0.8	12
7	1999/9/20 17:48:43.1	23.930	120.986	14.8	5.3	0.12	0.4	0.4	16
8	1999/9/20 17:49:03.1	23.993	120.791	7.0	5.2	0.13	0.2	0.2	25
9	1999/9/20 17:49:04.0	23.661	120.631	0.8	4.7	0.27	0.7	2.9	8
10	1999/9/20 17:49:21.6	23.969	120.942	11.3	4.8	0.21	0.8	0.5	12
11	1999/9/20 17:49:27.9	23.824	120.819	6.4	4.5	0.23	1.1	0.9	10
12	1999/9/20 17:49:31.2	23.665	120.715	7.1	4.8	0.11	0.5	0.8	8
13	1999/9/20 17:49:40.4	23.966	120.786	6.3	5.6	0.21	0.2	0.1	37
14	1999/9/20 17:50:00.6	23.965	120.857	7.6	4.8	0.13	0.4	0.4	12
15	1999/9/20 17:50:08.4	23.648	120.621	3.4	4.4	0.22	0.7	0.5	8
16	1999/9/20 17:50:23.2	23.600	120.653	5.9	4.5	0.10	0.5	0.3	8
17	1999/9/20 17:50:30.8	23.907	120.840	7.1	5.0	0.10	0.4	0.4	22
18	1999/9/20 17:50:35.5	23.819	120.855	7.7	5.3	0.06	0.3	0.2	12
19	1999/9/20 17:50:40.4	23.969	120.779	7.6	5.3	0.15	0.2	0.2	36
20	1999/9/20 17:50:56.0	24.049	120.887	7.4	4.2	0.19	0.4	0.8	10
21	1999/9/20 17:51:02.3	23.671	120.736	8.3	4.8	0.15	0.4	1.0	12
22	1999/9/20 17:51:08.8	23.923	120.991	12.4	4.7	0.11	0.7	0.5	16
23	1999/9/20 17:51:15.3	23.925	120.991	12.4	4.8	0.15	0.6	0.4	18
24	1999/9/20 17:51:25.9	23.597	120.646	4.4	4.8	0.19	0.5	0.3	10
25	1999/9/20 17:51:35.1	24.154	121.010	8.3	5.8	0.30	0.4	0.4	37
26	1999/9/20 17:51:60.0	24.002	120.880	10.8	4.7	0.24	0.5	0.8	11
27	1999/9/20 17:52:01.4	23.889	120.885	4.0	4.3	0.30	1.2	1.0	9
28	1999/9/20 17:52:05.5	23.934	120.940	10.5	5.1	0.13	0.4	0.3	27
29	1999/9/20 17:52:23.0	23.976	120.784	6.0	4.6	0.15	0.3	0.2	17
30	1999/9/20 17:52:24.1	24.068	120.836	8.4	4.6	0.24	0.5	0.4	10
31	1999/9/20 17:52:33.4	23.980	120.797	6.8	4.7	0.10	0.2	0.1	15
32	1999/9/20 17:52:35.7	23.976	120.850	11.7	4.8	0.19	0.6	0.6	12
33	1999/9/20 17:52:42.9	24.026	120.809	7.8	5.1	0.16	0.2	0.2	29
34	1999/9/20 17:52:47.3	23.939	120.845	9.9	4.8	0.19	0.3	0.4	9
35	1999/9/20 17:52:51.8	23.983	120.875	11.4	4.9	0.11	0.5	0.4	16
36	1999/9/20 17:53:01.7	23.673	120.624	2.5	4.3	0.05	0.7	0.7	8
37	1999/9/20 17:53:09.4	23.955	120.901	9.7	4.6	0.11	0.3	0.3	13
38	1999/9/20 17:53:11.6	23.954	120.882	10.7	4.9	0.17	0.4	0.5	31
39	1999/9/20 17:53:27.8	23.949	120.803	7.2	4.7	0.29	0.3	0.4	25
40	1999/9/20 17:53:35.1	23.985	120.851	10.6	4.3	0.23	0.6	0.7	12
41	1999/9/20 17:53:38.6	24.188	120.904	8.0	4.8	0.23	0.5	0.2	9
42	1999/9/20 17:53:39.8	23.748	120.773	4.3	4.7	0.10	0.2	0.2	22
43	1999/9/20 17:53:50.2	23.635	120.630	3.7	4.1	0.16	0.5	0.3	8
44	1999/9/20 17:54:04.0	23.866	120.824	6.6	4.0	0.21	0.5	0.8	10
45	1999/9/20 17:54:16.6	23.994	120.920	11.6	4.4	0.17	0.8	0.7	18
46	1999/9/20 17:54:24.9	23.916	120.988	12.7	4.6	0.20	0.7	0.7	13
47	1999/9/20 17:54:27.5	24.101	120.914	3.8	4.6	0.25	0.9	1.4	17
48	1999/9/20 17:54:37.6	23.990	120.965	9.7	4.1	0.10	0.4	0.2	7
49	1999/9/20 17:54:41.5	23.903	120.823	8.5	4.5	0.07	0.2	0.4	16
50	1999/9/20 17:54:44.2	23.908	120.901	11.6	4.6	0.14	0.4	0.3	24
51	1999/9/20 17:54:56.8	23.920	120.954	14.6	4.7	0.20	2.2	1.9	10
52	1999/9/20 17:55:04.4	23.956	120.903	11.7	4.5	0.13	0.3	0.3	16
53	1999/9/20 17:55:08.3	23.631	120.674	8.6	4.4	0.16	1.0	0.8	12
54	1999/9/20 17:55:14.6	23.956	120.937	12.6	4.8	0.15	0.6	0.4	13
55	1999/9/20 17:55:16.9	23.993	120.955	11.8	4.7	0.20	1.2	0.8	20
56	1999/9/20 17:55:21.2	23.843	120.829	8.9	4.5	0.07	0.3	0.4	9
57	1999/9/20 17:55:23.3	24.229	121.309	16.9	5.3	0.50	0.6	1.6	19
58	1999/9/20 17:55:34.7	23.936	120.859	8.8	4.5	0.26	0.5	0.9	10
59	1999/9/20 17:55:39.0	23.967	120.779	6.6	4.8	0.14	0.2	0.2	28
60	1999/9/20 17:55:56.1	23.856	120.813	6.0	4.6	0.12	0.2	0.2	22

(*continued*)

Table 1
Continued

No.	Origin Time (UT)	Latitude (° N)	Longitude (° E)	Depth (km)	M_L	RMS* (sec)	ERH† (km)	ERZ‡ (km)	No. Arrivals
61	1999/9/20 17:56:00.6	23.924	120.969	13.8	4.8	0.14	0.4	0.3	23
62	1999/9/20 17:56:02.2	23.640	120.676	8.3	4.5	0.10	0.6	0.4	8
63	1999/9/20 17:56:09.2	23.776	120.868	5.1	4.2	0.33	1.4	0.7	8
64	1999/9/20 17:56:10.7	23.922	120.908	10.8	4.2	0.08	0.6	0.5	6
65	1999/9/20 17:56:15.5	23.974	120.782	5.6	4.6	0.22	0.3	0.2	14
66	1999/9/20 17:56:23.8	23.933	120.786	3.8	4.3	0.20	0.3	0.6	16
67	1999/9/20 17:56:33.7	23.949	120.816	7.1	4.9	0.14	0.4	0.4	28
68	1999/9/20 17:56:53.0	23.810	120.831	8.3	4.9	0.17	0.3	0.2	30
69	1999/9/20 17:56:56.1	24.141	120.915	1.8	4.5	0.10	0.3	0.7	11
70	1999/9/20 17:57:01.3	23.824	120.852	7.6	4.5	0.08	0.4	0.3	14
71	1999/9/20 17:57:09.2	23.641	120.687	8.7	4.4	0.06	0.4	0.5	8
72	1999/9/20 17:57:11.3	23.869	120.862	9.5	4.8	0.14	0.5	0.3	16
73	1999/9/20 17:57:13.9	23.866	120.813	4.8	4.6	0.18	0.4	1.0	10
74	1999/9/20 17:57:15.8	23.938	121.007	14.4	6.1	0.17	0.2	0.2	36
75	1999/9/20 17:57:37.2	24.070	120.909	8.4	4.9	0.10	0.3	0.3	12
76	1999/9/20 17:58:01.7	23.881	120.896	10.7	4.7	0.09	0.7	0.4	6
77	1999/9/20 17:58:10.1	23.914	120.770	0.6	4.4	0.13	0.2	0.7	18
78	1999/9/20 17:58:18.7	24.017	120.918	8.5	4.7	0.08	0.2	0.3	12
79	1999/9/20 17:58:22.3	24.013	120.796	7.1	4.8	0.17	0.5	0.3	9
80	1999/9/20 17:58:24.9	23.911	120.818	5.4	4.7	0.15	0.3	0.6	14
81	1999/9/20 17:58:28.0	23.628	120.670	6.1	4.4	0.04	0.3	0.1	6
82	1999/9/20 17:58:32.3	24.013	120.936	10.2	4.3	0.08	0.3	0.2	12
83	1999/9/20 17:58:32.6	23.858	120.809	5.1	4.3	0.07	0.2	0.3	10
84	1999/9/20 17:58:36.8	23.861	120.812	5.7	4.4	0.04	0.1	0.1	12
85	1999/9/20 17:58:45.0	24.220	121.113	10.8	5.5	0.16	0.7	0.6	10
86	1999/9/20 17:58:55.2	23.943	121.029	14.8	5.6	0.18	0.3	0.2	38
87	1999/9/20 17:59:18.5	23.854	120.785	6.2	4.8	0.21	0.4	0.8	26
88	1999/9/20 17:59:26.9	24.095	120.914	6.9	4.7	0.09	0.2	0.4	11
89	1999/9/20 17:59:30.1	23.869	120.834	5.4	4.7	0.08	0.1	0.2	23
90	1999/9/20 17:59:31.4	24.108	120.907	4.0	5.2	0.10	0.3	0.8	12
91	1999/9/20 17:59:36.3	23.923	120.918	10.2	4.7	0.13	0.5	0.5	14
92	1999/9/20 18:00:11.2	23.918	120.779	6.7	4.2	0.10	0.4	0.4	10
93	1999/9/20 18:00:14.8	23.921	120.914	7.3	4.3	0.11	1.3	0.3	6
94	1999/9/20 18:00:15.8	24.011	120.757	3.7	3.7	0.10	0.7	1.0	6
95	1999/9/20 18:00:37.0	23.871	120.861	10.0	4.4	0.08	0.4	0.3	13
96	1999/9/20 18:00:41.2	23.980	120.805	7.1	4.3	0.05	0.1	0.1	15
97	1999/9/20 18:00:47.5	23.972	120.785	6.1	4.4	0.10	0.2	0.1	18
98	1999/9/20 18:00:50.5	23.895	120.961	9.3	4.3	0.09	0.8	0.5	11
99	1999/9/20 18:00:58.1	23.938	120.970	15.2	4.8	0.10	0.3	0.3	20
100	1999/9/20 18:01:19.8	23.814	120.780	5.4	4.2	0.04	0.2	0.2	8
101	1999/9/20 18:01:31.7	23.902	120.913	9.9	3.9	0.11	0.4	0.3	10
102	1999/9/20 18:01:36.0	23.968	120.817	7.3	4.3	0.08	0.1	0.1	20
103	1999/9/20 18:01:56.6	23.992	120.965	10.3	3.9	0.10	0.5	0.3	8
104	1999/9/20 18:02:05.8	23.890	120.905	11.3	4.0	0.17	0.7	0.4	10
105	1999/9/20 18:02:11.9	23.967	120.881	10.6	4.4	0.18	0.3	0.4	25
106	1999/9/20 18:02:15.6	23.857	120.816	6.3	4.2	0.06	0.2	0.3	10
107	1999/9/20 18:02:19.8	24.228	121.098	8.5	5.4	0.17	0.1	0.1	28
108	1999/9/20 18:02:34.3	24.046	120.828	7.6	5.0	0.14	0.2	0.2	28
109	1999/9/20 18:03:18.1	23.965	120.979	17.1	4.4	0.20	0.9	0.3	17
110	1999/9/20 18:03:41.3	23.801	120.869	8.3	6.4	0.24	0.2	0.2	37
111	1999/9/20 18:03:53.5	23.971	120.789	5.1	5.8	0.24	0.3	0.2	32
112	1999/9/20 18:04:10.1	24.148	120.983	9.2	5.3	0.23	0.6	0.6	21
113	1999/9/20 18:04:23.2	23.819	120.858	7.5	4.7	0.04	0.2	0.1	8
114	1999/9/20 18:04:27.8	23.951	120.824	5.9	4.7	0.15	0.3	0.4	18
115	1999/9/20 18:04:37.3	23.982	120.805	6.7	4.4	0.28	0.6	0.3	12
116	1999/9/20 18:04:42.0	23.932	121.042	11.1	5.6	0.18	0.5	0.4	34
117	1999/9/20 18:04:42.5	23.632	120.688	8.9	4.7	0.15	0.7	0.5	8
118	1999/9/20 18:05:02.2	23.826	120.851	7.4	4.3	0.04	0.2	0.1	9
119	1999/9/20 18:05:15.0	23.951	120.996	11.2	4.9	0.10	0.4	0.2	17
120	1999/9/20 18:05:26.4	23.981	120.777	5.9	4.6	0.16	0.2	0.1	16

(*continued*)

Table 1
Continued

No.	Origin Time (UT)	Latitude (° N)	Longitude (° E)	Depth (km)	M_L	RMS* (sec)	ERH† (km)	ERZ‡ (km)	No. Arrivals
121	1999/9/20 18:05:29.1	23.831	120.842	6.6	4.2	0.06	0.7	0.2	6
122	1999/9/20 18:05:41.1	23.819	120.854	7.3	4.3	0.04	0.2	0.1	8
123	1999/9/20 18:05:53.3	23.955	120.779	6.7	5.4	0.24	0.1	0.1	34
124	1999/9/20 18:06:22.3	23.871	120.824	6.6	4.5	0.05	0.2	0.3	11
125	1999/9/20 18:06:30.8	23.833	120.852	7.0	4.0	0.12	0.6	0.4	6
126	1999/9/20 18:06:43.1	23.722	120.759	8.4	4.5	0.15	0.5	0.6	16
127	1999/9/20 18:06:43.9	23.975	120.934	11.9	4.4	0.10	0.5	0.3	14
128	1999/9/20 18:06:60.0	23.874	120.848	5.8	4.1	0.15	0.5	0.7	10
129	1999/9/20 18:07:09.5	24.123	120.917	6.8	4.2	0.22	0.4	0.4	12
130	1999/9/20 18:07:10.1	23.615	120.659	4.3	4.6	0.10	1.3	0.5	7
131	1999/9/20 18:07:11.1	23.874	120.866	9.0	4.3	0.07	0.4	0.3	12
132	1999/9/20 18:07:29.8	23.962	120.895	6.3	3.7	0.30	1.3	2.5	10
133	1999/9/20 18:07:30.3	23.832	120.845	7.4	3.9	0.16	0.9	0.4	9
134	1999/9/20 18:07:44.0	24.005	120.781	6.1	4.5	0.28	0.4	0.3	13
135	1999/9/20 18:07:45.0	23.919	120.981	10.8	4.5	0.16	0.8	0.3	15
136	1999/9/20 18:07:54.3	23.800	120.868	9.0	4.3	0.10	0.5	0.2	7
137	1999/9/20 18:08:01.8	23.862	120.892	8.2	4.2	0.15	0.7	0.5	12
138	1999/9/20 18:08:09.2	23.896	120.831	5.8	4.0	0.04	0.2	0.2	8
139	1999/9/20 18:08:13.8	23.974	120.971	10.1	4.3	0.10	0.5	0.3	10
140	1999/9/20 18:08:14.5	23.854	120.856	8.0	4.2	0.06	0.4	0.3	7
141	1999/9/20 18:08:14.5	23.980	120.767	4.6	4.7	0.16	0.2	0.1	28
142	1999/9/20 18:08:31.0	23.981	120.939	11.0	4.6	0.18	0.4	0.3	21
143	1999/9/20 18:08:46.3	23.896	120.898	10.1	4.5	0.07	0.4	0.2	15
144	1999/9/20 18:08:49.7	24.080	120.942	7.4	4.3	0.07	0.2	0.3	9
145	1999/9/20 18:09:08.5	23.833	120.838	6.2	4.3	0.17	0.8	0.5	10
146	1999/9/20 18:09:13.9	23.875	120.757	6.0	4.7	0.27	0.2	0.4	32
147	1999/9/20 18:09:24.8	23.993	121.081	3.0	4.5	0.19	0.5	1.8	10
148	1999/9/20 18:09:32.3	23.978	120.953	13.6	4.6	0.17	0.7	0.5	25
149	1999/9/20 18:09:47.3	24.009	120.773	6.6	4.1	0.17	0.5	0.3	10
150	1999/9/20 18:09:49.3	24.290	121.111	2.1	4.5	0.16	1.6	2.7	7
151	1999/9/20 18:09:52.5	24.003	120.782	5.8	4.2	0.09	0.2	0.1	12
152	1999/9/20 18:09:53.6	23.878	120.824	6.6	4.2	0.13	0.3	0.6	10
153	1999/9/20 18:09:57.0	23.910	120.837	8.7	4.3	0.09	0.3	0.3	19
154	1999/9/20 18:10:01.4	23.874	120.808	3.4	4.0	0.16	0.3	0.8	9
155	1999/9/20 18:10:04.7	23.960	121.018	6.5	4.0	0.25	0.5	0.4	14
156	1999/9/20 18:10:18.5	24.021	120.927	9.0	4.0	0.08	0.4	0.2	9
157	1999/9/20 18:10:28.9	24.012	120.933	10.0	4.0	0.16	0.5	0.4	10
158	1999/9/20 18:10:37.3	24.028	120.933	8.8	4.1	0.04	0.2	0.2	11
159	1999/9/20 18:10:45.0	24.087	120.951	9.0	4.7	0.08	0.2	0.2	11
160	1999/9/20 18:10:50.8	23.958	120.785	6.3	4.4	0.08	0.3	0.3	12
161	1999/9/20 18:10:55.0	23.847	120.805	3.8	4.2	0.07	0.6	0.6	8
162	1999/9/20 18:11:19.4	23.835	120.582	12.9	4.4	0.03	0.7	0.5	8
163	1999/9/20 18:11:27.0	23.973	120.975	11.1	5.0	0.16	0.1	0.1	22
164	1999/9/20 18:11:36.8	24.265	121.128	14.1	6.1	0.17	0.6	0.2	16
165	1999/9/20 18:11:38.4	23.978	120.785	5.9	5.1	0.18	0.4	0.1	11
166	1999/9/20 18:11:53.7	23.881	121.060	30.1	6.6	0.39	0.6	0.4	36
167	1999/9/20 18:11:54.3	24.001	120.926	10.7	5.4	0.11	0.4	0.3	13
168	1999/9/20 18:12:01.7	23.662	120.647	1.2	4.9	0.15	4.1	2.1	6
169	1999/9/20 18:12:46.9	24.049	120.949	8.9	4.5	0.04	0.2	0.1	8
170	1999/9/20 18:13:02.3	23.978	120.799	6.8	4.7	0.15	0.4	0.2	19
171	1999/9/20 18:13:09.3	24.022	120.834	8.9	4.8	0.09	0.3	0.2	10
172	1999/9/20 18:13:11.5	24.047	120.783	5.6	4.7	0.10	0.2	0.4	14
173	1999/9/20 18:13:35.5	23.913	120.638	14.5	4.4	0.14	1.7	0.8	9
174	1999/9/20 18:13:35.8	23.604	120.608	3.9	4.5	0.21	0.5	0.2	7
175	1999/9/20 18:13:41.2	23.863	120.803	7.7	4.4	0.19	0.3	0.7	24
176	1999/9/20 18:13:42.8	24.173	121.047	8.5	4.7	0.10	0.8	0.7	7
177	1999/9/20 18:13:50.4	23.938	121.006	9.2	4.8	0.13	0.4	0.6	23
178	1999/9/20 18:13:57.8	23.906	120.873	9.6	4.6	0.08	0.9	0.5	9
179	1999/9/20 18:13:59.0	23.731	120.865	12.4	4.9	0.20	0.9	1.0	24
180	1999/9/20 18:14:14.6	24.002	120.789	8.1	4.2	0.27	0.6	0.3	11

(*continued*)

Table 1
Continued

No.	Origin Time (UT)	Latitude (° N)	Longitude (° E)	Depth (km)	M_L	RMS* (sec)	ERH† (km)	ERZ‡ (km)	No. Arrivals
181	1999/9/20 18:14:22.6	23.903	120.806	5.3	4.0	0.10	0.2	0.5	14
182	1999/9/20 18:14:32.0	23.873	120.823	1.4	4.1	0.23	0.3	1.0	15
183	1999/9/20 18:14:45.5	23.979	120.794	6.8	4.2	0.15	0.4	0.2	11
184	1999/9/20 18:14:51.2	23.947	120.810	6.7	4.3	0.13	0.2	0.3	15
185	1999/9/20 18:15:10.3	23.578	120.666	12.1	4.8	0.12	0.7	0.4	9
186	1999/9/20 18:15:15.1	23.863	120.807	7.7	4.3	0.42	0.6	1.1	14
187	1999/9/20 18:15:18.7	23.612	120.657	4.9	4.4	0.14	0.5	0.4	9
188	1999/9/20 18:15:36.1	23.829	120.832	6.4	4.3	0.10	0.5	0.3	10
189	1999/9/20 18:15:39.2	24.059	120.926	8.6	4.3	0.09	0.2	0.3	14
190	1999/9/20 18:15:43.3	23.670	120.952	16.0	5.4	0.16	0.1	0.1	25
191	1999/9/20 18:15:48.0	24.008	120.941	12.7	4.5	0.16	0.5	0.4	14
192	1999/9/20 18:16:17.3	23.864	121.065	22.3	6.7	0.27	0.4	0.2	35
193	1999/9/20 18:16:47.1	23.923	121.056	10.5	5.3	0.09	0.7	0.6	15
194	1999/9/20 18:17:00.7	23.910	121.021	17.6	5.4	0.11	0.3	0.1	26
195	1999/9/20 18:17:07.7	24.025	120.846	3.2	5.1	0.58	1.0	1.4	18
196	1999/9/20 18:17:20.1	23.884	120.923	12.3	5.1	0.13	0.4	0.3	36
197	1999/9/20 18:17:37.0	23.844	120.919	11.2	4.4	0.32	1.2	0.8	16
198	1999/9/20 18:17:47.6	23.958	120.910	11.6	4.2	0.19	0.8	0.9	12
199	1999/9/20 18:17:48.9	23.740	120.765	6.3	4.6	0.13	0.5	1.1	12
200	1999/9/20 18:18:04.9	23.933	120.860	12.2	4.2	0.04	0.1	0.2	8
201	1999/9/20 18:18:15.3	23.920	121.033	25.3	4.8	0.19	1.1	0.7	22
202	1999/9/20 18:18:33.2	23.815	120.768	7.8	4.4	0.13	0.4	0.4	14
203	1999/9/20 18:18:39.2	23.860	120.787	2.9	5.2	0.20	0.1	0.4	33
204	1999/9/20 18:18:45.3	23.649	120.668	2.5	4.6	0.07	0.6	1.0	7
205	1999/9/20 18:18:52.8	23.861	120.933	11.7	4.8	0.09	0.4	0.3	27
206	1999/9/20 18:18:53.1	23.725	120.726	17.4	4.8	0.17	0.7	0.9	16
207	1999/9/20 18:19:10.9	23.861	120.872	10.1	4.4	0.11	0.4	0.2	14
208	1999/9/20 18:19:16.1	23.971	120.769	7.0	4.2	0.20	0.6	0.3	14
209	1999/9/20 18:19:17.9	24.175	120.914	3.8	3.9	0.14	0.3	0.2	8
210	1999/9/20 18:19:22.7	23.586	120.656	4.1	4.5	0.15	0.8	0.3	8
211	1999/9/20 18:19:28.0	23.901	121.125	12.8	4.8	0.22	0.9	1.1	16
212	1999/9/20 18:20:14.9	23.939	121.033	15.3	4.2	0.06	0.5	0.2	7
213	1999/9/20 18:20:18.4	23.847	120.846	6.9	4.1	0.04	0.1	0.2	9
214	1999/9/20 18:20:31.5	24.115	121.013	9.3	4.9	0.20	0.2	0.4	28
215	1999/9/20 18:20:40.1	23.933	121.026	26.7	4.9	0.10	0.6	0.5	13
216	1999/9/20 18:20:46.3	23.924	121.059	14.6	4.5	0.12	0.9	0.6	11
217	1999/9/20 18:20:46.3	23.627	120.608	3.5	4.2	0.19	0.3	0.5	6
218	1999/9/20 18:20:51.5	24.060	120.889	8.3	4.2	0.14	0.4	0.3	11
219	1999/9/20 18:20:57.2	23.926	120.926	11.3	4.7	0.13	0.3	0.2	21
220	1999/9/20 18:21:23.0	24.014	120.946	10.7	4.3	0.19	0.8	0.4	14
221	1999/9/20 18:21:28.8	23.996	121.048	11.1	5.3	0.19	0.2	0.1	34
222	1999/9/20 18:21:50.6	23.865	120.903	11.0	4.3	0.16	0.8	0.4	10
223	1999/9/20 18:21:58.7	23.977	120.794	6.8	4.2	0.07	0.2	0.2	24
224	1999/9/20 18:22:05.3	23.862	121.045	22.0	5.1	0.16	0.2	0.3	35
225	1999/9/20 18:22:20.5	23.891	121.092	13.7	5.2	0.10	0.9	0.8	14
226	1999/9/20 18:22:27.6	23.960	120.917	10.7	5.0	0.16	0.2	0.2	32
227	1999/9/20 18:22:35.8	24.032	120.941	9.4	4.5	0.12	0.6	0.5	15
228	1999/9/20 18:23:01.4	23.927	120.917	11.6	3.9	0.07	0.4	0.3	6
229	1999/9/20 18:23:25.0	23.858	120.870	9.3	4.4	0.12	0.5	0.3	20
230	1999/9/20 18:23:36.6	23.843	120.842	9.2	4.4	0.15	0.4	0.3	22
231	1999/9/20 18:23:50.8	24.028	120.942	10.5	4.2	0.08	0.3	0.2	15
232	1999/9/20 18:23:52.2	23.869	120.830	6.3	3.6	0.04	0.2	0.2	8
233	1999/9/20 18:23:53.5	23.866	120.775	0.5	4.1	0.03	0.2	0.4	10
234	1999/9/20 18:24:01.3	24.001	120.781	9.1	3.9	0.12	0.6	0.2	10
235	1999/9/20 18:24:03.0	23.866	120.808	5.1	3.9	0.08	0.2	0.4	12
236	1999/9/20 18:24:09.3	23.841	120.992	16.6	4.3	0.16	0.7	0.7	10
237	1999/9/20 18:24:16.2	23.900	120.802	5.7	4.0	0.08	0.2	0.4	16
238	1999/9/20 18:24:24.8	23.856	120.921	20.5	3.8	0.23	0.8	2.5	14
239	1999/9/20 18:24:33.6	23.065	120.200	13.2	3.8	0.22	0.7	0.3	8
240	1999/9/20 18:24:35.0	23.821	120.860	7.4	4.3	0.05	0.3	0.1	8

(*continued*)

Table 1
Continued

No.	Origin Time (UT)	Latitude (° N)	Longitude (° E)	Depth (km)	M_L	RMS* (sec)	ERH† (km)	ERZ‡ (km)	No. Arrivals
241	1999/9/20 18:24:48.3	23.961	120.781	6.2	4.0	0.06	0.3	0.2	10
242	1999/9/20 18:24:52.4	23.864	120.843	7.3	4.1	0.06	0.2	0.2	14
243	1999/9/20 18:24:58.0	23.838	120.908	16.3	4.6	0.28	1.8	1.0	15
244	1999/9/20 18:25:02.0	23.826	120.802	8.9	4.7	0.21	0.2	0.2	28
245	1999/9/20 18:25:16.3	24.017	121.015	7.4	3.7	0.02	0.2	0.1	6
246	1999/9/20 18:25:23.1	23.961	120.756	6.3	4.0	0.05	0.5	0.2	7
247	1999/9/20 18:25:37.3	24.116	121.007	9.1	4.4	0.39	0.8	1.2	10
248	1999/9/20 18:25:43.0	24.045	120.789	7.8	4.1	0.09	0.3	0.4	6
249	1999/9/20 18:25:45.5	23.661	120.959	16.3	5.2	0.17	0.2	0.2	30
250	1999/9/20 18:26:10.4	23.856	120.865	8.6	5.3	0.16	0.1	0.1	32
251	1999/9/20 18:26:34.3	23.987	120.966	11.5	4.6	0.12	0.4	0.3	18
252	1999/9/20 18:26:59.5	23.929	120.922	7.4	3.9	0.10	0.2	0.4	16
253	1999/9/20 18:27:14.0	23.930	120.930	11.9	4.6	0.22	0.3	0.2	22
254	1999/9/20 18:27:23.5	23.869	120.858	8.1	4.1	0.04	0.3	0.3	12
255	1999/9/20 18:27:36.2	23.694	121.424	9.0	3.4	0.30	1.1	1.0	8
256	1999/9/20 18:28:02.5	23.848	121.015	18.2	5.3	0.17	0.2	0.1	36
257	1999/9/20 18:28:25.2	23.991	120.942	8.9	3.8	0.06	0.3	0.2	9
258	1999/9/20 18:28:34.3	23.906	120.843	6.5	4.1	0.16	0.4	0.6	8
259	1999/9/20 18:29:07.2	23.843	120.836	6.9	3.8	0.16	0.4	0.4	8
260	1999/9/20 18:29:26.9	23.711	121.473	13.9	3.8	0.24	0.4	0.3	13
261	1999/9/20 18:29:29.0	23.851	120.880	10.5	4.4	0.19	0.5	0.4	12
262	1999/9/20 18:29:31.8	23.883	120.905	15.3	4.4	0.30	1.0	1.2	16
263	1999/9/20 18:29:59.7	24.071	120.951	8.9	4.8	0.18	0.2	0.1	20
264	1999/9/20 18:30:26.8	23.953	120.890	11.0	4.4	0.15	0.4	0.5	18
265	1999/9/20 18:30:42.7	23.898	120.820	3.7	3.7	0.07	0.2	0.2	12
266	1999/9/20 18:30:48.6	23.905	121.313	0.9	3.5	0.24	1.6	3.4	8
267	1999/9/20 18:31:08.2	23.936	120.966	12.9	4.4	0.16	0.8	0.5	14
268	1999/9/20 18:31:08.5	24.216	120.991	8.2	4.0	0.06	0.3	0.2	6
269	1999/9/20 18:31:25.6	23.867	120.847	8.1	4.3	0.03	0.2	0.2	6
270	1999/9/20 18:31:39.9	23.850	120.888	9.7	4.1	0.12	0.6	0.3	9
271	1999/9/20 18:31:56.3	24.122	120.884	10.7	4.7	0.13	0.5	0.4	20
272	1999/9/20 18:32:21.1	23.912	120.783	2.4	4.1	0.16	0.5	1.5	12
273	1999/9/20 18:32:21.9	24.072	120.937	7.1	4.1	0.10	0.4	0.3	10
274	1999/9/20 18:32:44.9	23.921	120.822	7.2	4.3	0.11	0.3	0.3	14
275	1999/9/20 18:32:55.1	23.838	121.002	17.4	5.2	0.17	0.2	0.2	31
276	1999/9/20 18:33:10.1	23.893	120.820	5.9	4.4	0.06	0.3	0.3	16
277	1999/9/20 18:33:19.4	23.980	120.866	15.6	4.5	0.29	1.6	2.1	9
278	1999/9/20 18:33:34.5	24.033	120.805	8.5	3.8	0.09	0.4	0.3	8
279	1999/9/20 18:34:03.8	23.943	120.887	10.1	3.8	0.03	0.1	0.1	8
280	1999/9/20 18:34:25.9	23.852	121.035	22.1	5.0	0.18	0.3	0.3	28
281	1999/9/20 18:34:26.5	23.988	120.793	7.3	4.0	0.17	0.3	0.2	9
282	1999/9/20 18:35:35.5	24.210	121.132	9.6	4.8	0.14	0.1	0.1	12
283	1999/9/20 18:35:40.2	23.977	120.767	6.3	4.1	0.15	0.3	0.2	12
284	1999/9/20 18:35:52.2	23.858	120.883	9.4	4.8	0.29	0.2	0.2	28
285	1999/9/20 18:36:17.6	23.627	120.679	3.0	4.3	0.05	0.7	0.3	6
286	1999/9/20 18:37:11.9	24.053	120.780	4.9	4.7	0.17	0.1	0.1	19
287	1999/9/20 18:37:32.9	24.063	120.943	8.9	3.8	0.08	0.3	0.3	8
288	1999/9/20 18:37:37.3	23.990	121.056	7.1	3.9	0.02	0.1	0.1	6
289	1999/9/20 18:37:44.9	23.867	120.882	7.9	4.4	0.17	0.5	0.4	14
290	1999/9/20 18:37:50.2	23.947	121.022	13.3	4.5	0.17	0.3	0.2	13
291	1999/9/20 18:38:24.6	23.867	120.863	7.8	4.4	0.06	0.2	0.2	16
292	1999/9/20 18:38:36.9	23.520	120.831	6.2	3.5	0.18	1.3	0.3	14
293	1999/9/20 18:39:15.5	23.930	120.961	11.9	4.8	0.15	0.2	0.1	20
294	1999/9/20 18:39:23.6	23.959	120.899	12.6	4.4	0.11	0.4	0.5	10
295	1999/9/20 18:39:27.0	23.904	120.912	10.6	4.3	0.02	0.1	0.1	6
296	1999/9/20 18:39:47.5	23.541	120.609	0.6	3.5	0.17	2.5	1.7	6

*rms, 0.15 ± 0.079 sec in average.
†ERH, 0.49 ± 0.403 km in average.
‡ERZ, 0.47 ± 0.456 km in average.

Table 2
Focal Mechanisms of the 24 Aftershocks Determined in This Study

No.	Origin Time (UT)	Latitude (° N)	Longitude (° E)	Depth (km)	M_L	Strike1 Strike2	Dip1 Dip2	Rake1 Rake2
1	1999/9/20 18:03:41.3	23.801	120.869	8.3	6.4	10.0	80.0	−130.0
						268.3	41.0	−15.3
2	1999/9/20 18:05:53.3	23.955	120.779	6.7	5.4	30.0	58.0	125.0
						157.1	46.0	47.5
3	1999/9/20 18:16:17.3	23.864	121.065	22.3	6.7	0.0	30.0	65.0
						208.3	63.1	103.7
4	1999/9/20 18:20:31.5	24.115	121.013	9.3	4.9	203.0	40.0	−25.0
						312.7	74.2	−127.3
5	1999/9/20 18:27:14.0	23.930	120.930	11.9	4.6	5.0	22.0	66.0
						210.7	70.0	99.3
6	1999/9/20 18:57:04.3	24.129	120.812	4.3	4.9	20.0	40.0	35.0
						261.8	68.4	124.5
7	1999/9/20 19:40:32.5	23.573	120.894	8.3	5.5	160.0	85.0	5.0
						69.6	85.0	175.0
8	1999/9/20 19:44:56.1	24.053	120.776	6.0	4.6	60.0	28.0	135.0
						191.4	70.6	69.4
9	1999/9/20 19:57:52.6	24.031	120.859	16.0	5.3	15.0	35.0	45.0
						245.7	66.1	116.3
10	1999/9/20 20:02:15.9	23.982	120.791	9.3	5.7	20.0	65.0	80.0
						222.6	26.8	110.4
11	1999/9/20 20:29:21.0	23.813	120.945	14.6	4.8	325.0	35.0	50.0
						190.7	63.9	114.2
12	1999/9/20 20:43:48.8	23.761	121.299	11.9	5.3	10.0	37.0	−105.0
						208.5	54.5	−79.0
13	1999/9/20 21:41:22.7	23.597	120.575	15.8	5.2	265.0	70.0	145.0
						8.5	57.4	24.0
14	1999/9/20 21:46:37.2	23.649	120.847	7.2	6.8	144.0	60.0	−5.0
						236.5	85.7	−149.9
15	1999/9/20 21:54:46.9	23.629	120.788	6.1	5.8	69.0	78.0	−105.0
						301.2	19.1	−39.4
16	1999/9/20 23:18:13.6	23.454	120.875	3.7	5.3	358.0	66.0	11.0
						263.5	80.0	155.6
17	1999/9/21 03:31:49.0	24.021	120.982	14.4	5.2	8.0	70.0	−40.0
						114.0	52.8	−154.6
18	1999/9/21 08:03:17.5	23.653	120.626	15.5	4.8	55.0	47.0	124.0
						190.3	52.7	59.1
19	1999/9/21 11:07:42.1	23.672	120.816	11.7	5.1	350.0	57.0	−10.0
						85.5	81.6	−146.6
20	1999/9/21 14:29:21.9	24.033	121.323	4.9	4.6	182.0	53.0	−16.0
						281.8	77.3	−141.9
21	1999/9/21 14:40:04.1	24.310	120.858	7.5	5.0	79.0	60.0	−135.0
						322.4	52.2	−39.2
22	1999/9/21 15:08:49.1	24.474	120.967	7.6	4.0	11.0	70.0	−20.0
						108.1	71.3	−158.8
23	1999/9/21 15:28:10.3	23.617	120.819	9.3	5.1	353.0	40.0	47.0
						223.6	62.0	119.8
24	1999/9/21 16:16:15.9	23.819	121.326	15.9	4.5	5.0	40.0	−105.0
						204.3	51.6	−77.7

dipping narrow zone, which may be associated with the Chi-Chi earthquake rupture zone. Some deeper events were located with focal depths >20 km and they most likely happened on a high-angle, west-dipping fault (e.g., Hirata *et al.*, 2000; Chen *et al.*, 2002; Lee *et al.*, 2002; Lin and Ando, 2004; Wu *et al.*, 2004). Also Figure 6c shows that the larger aftershocks tend to occur near the junction of the two conjugate faults (dashed lines in Fig. 6c) and along the west-dipping fault.

In Figure 7, epicenters of the 296 aftershocks determined in this study are plotted together with the mainshock slip distribution of Ma *et al.* (2001). Most of the mainshock

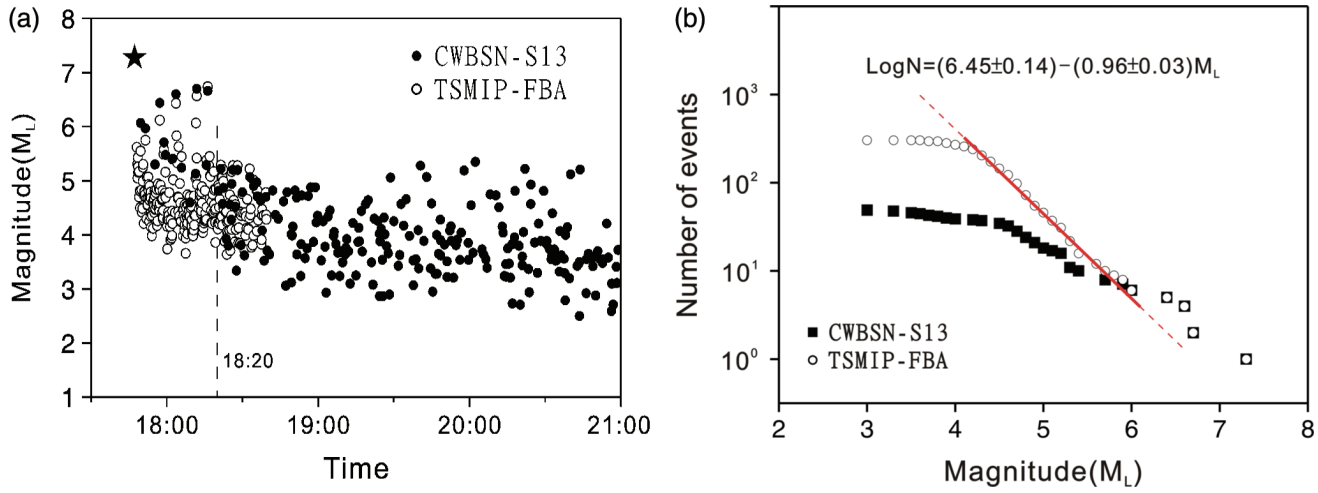

Figure 5. (a) Magnitudes of events in the Chi-Chi earthquake sequence versus time from the mainshock at 17:47 to 21:00 on 20 September 1999. The mainshock is indicated by the star. Open circles show the 296 events determined in this study using the TSMIP records, whereas filled circles are from the CWBSN catalog. Because of the failrue at many CWBSN stations, the CWBSN catalog is incomplete before about 18:20 indicated by the dashed line. (b) Gutenberg–Richter plot of the cumulative number of events determined in this study in the 1-hour time window after the Chi-Chi mainshock. The straight-line portion of the curve yields a *b*-value of nearly 1, while the flattening of the curve for M_L <4.3 is the result of the minimum magnitude cutoff by the TSMIP stations.

slip has been concentrated in the areas above the mainshock hypocenter (star), especially in two patches, one to the north and the other right above the hypocenter. As shown in Figure 6, the earliest aftershocks were mostly located at shallow depths within the small-slip region of the mainshock. Then, more aftershocks occurred at greater depths as the stress continued to be released across regions where there was little slip during the mainshock. The correlation between areas of high slip on a fault and low aftershock activity has been observed by Mendoza and Hartzell (1988), although definitive confirmation of this correlation has proved difficult because of the lack of reliable aftershock locations (e.g., Wald and Heaton 1994; Cohee and Beroza 1994). From the Chi-Chi earthquake sequence, Ma *et al.* (2001, 2005) revealed that there is a good correlation between slip-distribution and the aftershock locations determined by the CWBSN (mostly occurring after 18:20 on 20 September). The distribution of the 296 aftershocks within the first hour after the Chi-Chi earthquake determined in this study also confirms this proposition.

Conclusion

Although TSMIP was designed to record strong ground motion for hazard mitigation, its capability to record a broad magnitude range of earthquakes on scale allows the determination of detailed source behavior within the first hour of the M_W 7.6 Chi-Chi earthquake. Because of the numerous large aftershocks immediately following a big earthquake, it is quite a challenge to pick the arrival times of seismic phases and to associate them with the corresponding events. From our study we conclude that hundreds of $3 < M_L < 5$ events occurred in the crust around the main rupture within the first hour after the Chi-Chi mainshock. The spatial distribution of the aftershocks in the first hour following the Chi-Chi mainshock suggests that there is an expansion of aftershocks away from the high-slip locations. This rather short-term temporal change in aftershock distribution can only be seen from results obtained using near-source strong-motion records. After about one hour, aftershocks become less frequent, and within the day the aftershocks began to concentrate in the fringe area of the main rupture, a pattern after the Chi-Chi earthquake that persisted until 2003. Our result demonstrates that in a seismically active area with a potential for events of magnitude 7 or greater, the deployment of instruments capable of recording both the weak motions of small earthquakes as well as strong motions of the large events is necessary to trace the detailed and complete history of aftershock activity following a strong mainshock.

Acknowledgments

We wish to thank Jer-Ming Chiu and Naoshi Hirata for their invaluable comments that helped improve this article. This research has been supported by the National Science Council (NSC95-2119-M-043-MY3 and NSC95-2625-Z-002-028) with TEC contribution number 00002 and the Central Weather Bureau of the Republic of China (C.-H.C., Y.-M.W., and L.Z.), and the National Science Foundation (EAR0410227) (F.T.W.).

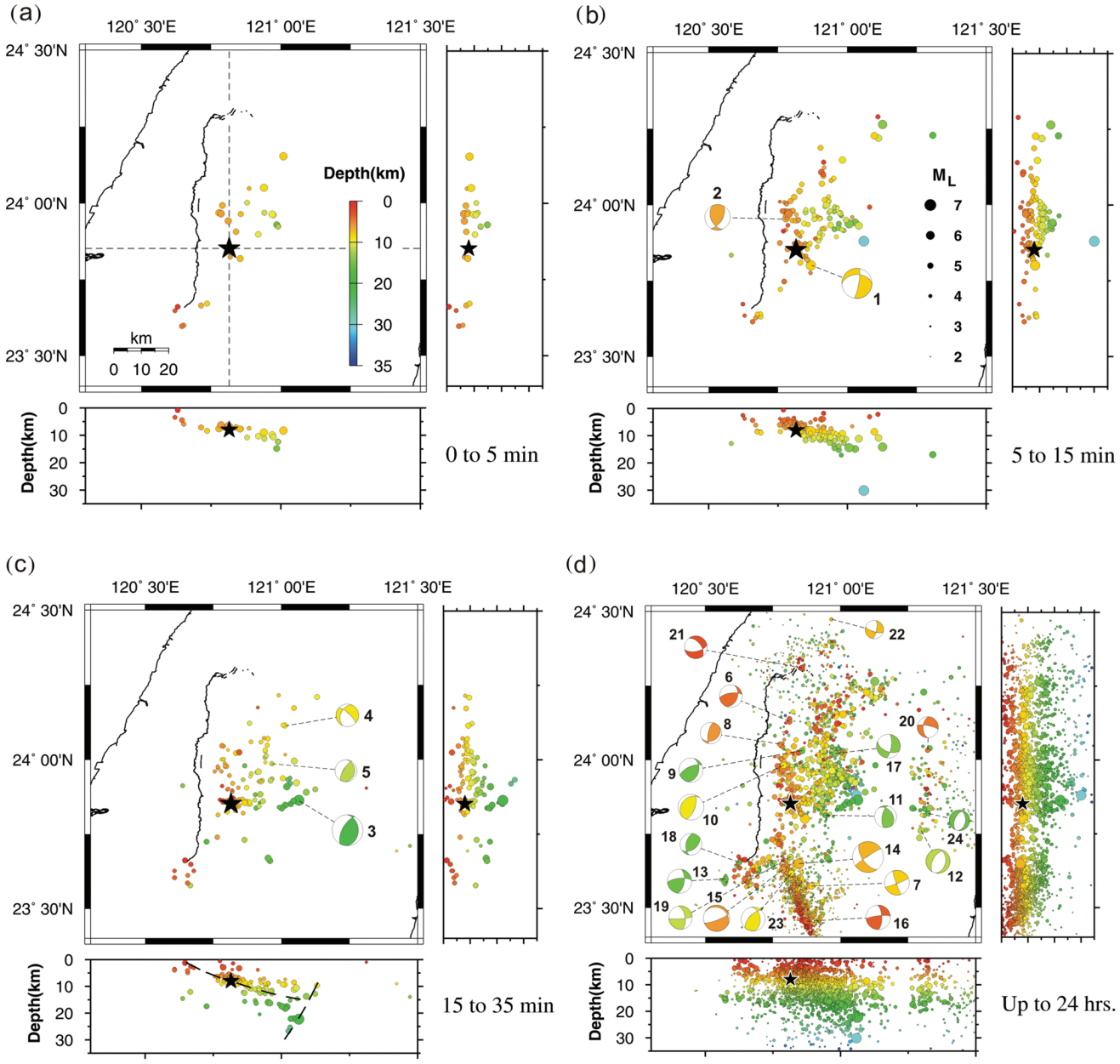

Figure 6. Hypocentral distribution and focal mechanisms of the Chi-Chi aftershocks from the occurrence of the mainshock up to four different times. (a), (b), and (c), all results are from this study, (d) Results from this study and from the CWBSN catalog are plotted. The two north–south and east–west vertical profiles in each figure are plotted by projecting all the events in the corresponding time window onto the vertical planes indicated by the dashed lines in (a). The mainshock is indicated by the star. The roughly north–south trending solid line indicates the surface rupture of the Chelungpu fault. Events are grouped into three depth ranges and plotted in different colors with their depths indicated by the color bar in (a). The sizes of the circles indicate the event magnitudes as indicated in (b). The dashed lines in (c) show the approximate locations of the two conjugate fault planes (see text). The beachballs in (b), (c), and (d) show the focal mechanisms of the 24 events determined in this study. The number associated with each beachball is the event's serial number in Table 2.

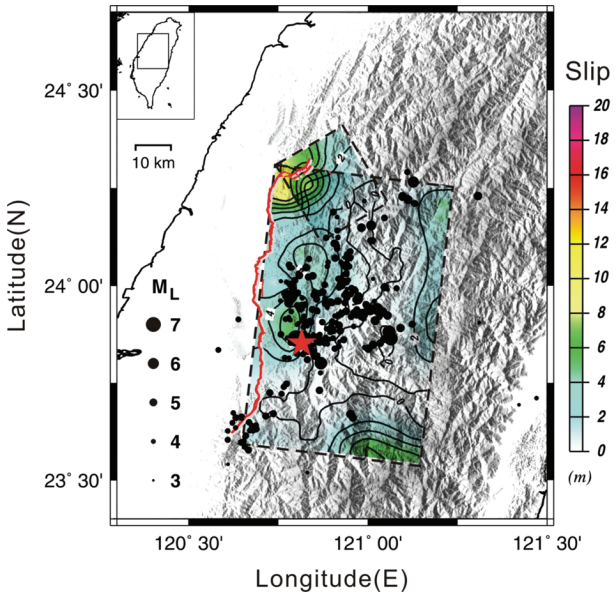

Figure 7. Epicenters of the 296 events determined in this study plotted over the slip distribution result of Ma *et al.* (2001). The Chi-Chi epicenter is indicated by the star. The color scheme represents the amount of slip in meters during the Chi-Chi mainshock. The sizes of the filled circles indicate the magnitude of the events.

References

Chang, C. H., Y. M Wu, T. C. Shin, and C. Y. Wang (2000). Relocating the 1999 Chi-Chi Earthquake, Taiwan, *Terr. Atmos. Ocean. Sci.* **11,** 581–590.

Chen, Y. G., W. S. Chen, J. C. Lee, Y. H. Lee, C. Y. Lee, H. C. Chang, and C. H. Lo (2001). Surface rupture of 1999 Chi-Chi earthquake yields insights on active tectonics of central Taiwan, *Bull. Seism. Soc. Am.* **91,** 977–985.

Chen, K. C., B. S. Huang, J. H. Wang, and H. Y. Yen (2002). Conjugate thrust faulting associated with the 1999 Chi-Chi, Taiwan, earthquake sequence, *Geophys. Res. Lett.* **29,** no. 8, 1277, doi 10.1029/2001GL014250.

Cohee, B. P., and G. C. Beroza (1994). Slip distribution of the 1992 Landers earthquake and its implications for earthquake source mechanics, *Bull. Seism. Soc. Am.* **84,** 692–712.

Flinn, E. A. (1965). Confidence regions and error determinations for seismic event location, *Rev. Geophys*. **3,** 157–185.

Helmstetter, A., Y. Y. Kagan, and D. D. Jackson (2005). Comparison of short-term and time-independent earthquake forecast models for Southern California, *Bull. Seism. Soc. Am.* **96,** 90–106.

Hirata, N., S. Sakai, Z. S. Liaw, Y. B. Tsai, and S. B. Yu (2000). Aftershock observation of the 1999 Chi-Chi, Taiwan earthquake, *Bull. Earthquake Res. Inst. Univ. Tokyo* **75,** 33–46.

Ji, C., D. V. Helmberger, D. J. Wald, and K. F. Ma (2003). Slip history and dynamic implications of the 1999 Chi-Chi, Taiwan, earthquake, *J. Geophys. Res.* **108,** 2412, doi 10.1029/2002JB001764.

Kao, H., and W. P. Chen (2000). The Chi-Chi earthquake sequence: Active, out-of-sequence thrust faulting in Taiwan, *Science* **288,** 2346–2349.

Lee, J. C., H. T. Chu, J. Angelier, Y. C. Chan, J. C. Hu, C. Y. Lu, and R. J. Rau (2002). Geometry and structure of northern surface ruptures of the 1999 Mw = 7.6 Chi-Chi, Taiwan, earthquake: influence from inherited fold belts structures, *J. Struct. Geol.* **24,** 173–192.

Lin, C. H., and M. Ando (2004). Seismological evidence of simultaneous mountain-building and crust-thickening from the 1999 Taiwan Chi-Chi earthquake (Mw = 7.6), *Earth Planets Space* **56,** 163–167.

Ma, K. F., C. H. Chan, and R. Stein (2005). Response of seismicity to Coulomb stress triggers and shadows of the 1999 Mw = 7.6 Chi-Chi, Taiwan, earthquake, *J. Geophys. Res.* **110,** B05S19, doi 10.1029/2004JB003389.

Ma, K. F., J. Mori, S. J. Lee, and S. B. Yu (2001). Spatial and temporal distribution of slip for the 1999 Chi-Chi, Taiwan, earthquake, *Bull. Seism. Soc. Am.* **91,** 1069–1087.

Mendoza, C., and S. H. Hartzell (1988). Aftershock patterns and main shock faulting, *Bull. Seism. Soc. Am.* **78,** 1438–1449.

Shin, T. C. (1993). The calculation of local magnitude from the simulated Wood-Anderson seismograms of the short-period seismograms, *Terr. Atmos. Ocean. Sci.* **4,** 155–170.

Thurber, C. H. (1993). Local earthquake tomography: velocities and Vp/Vs—theory, in *Seismic Tomography: Theory and Practice*, H. M. Iyer and K. Hirahara (Editors), Chapman & Hall, London, United Kingdom.

Thurber, C., and D. Eberhart-Phillips (1999). Local earthquake tomography with flexible gridding, *Comp. Geosci.* **25,** 809–818.

Wald, D. J., and T. H. Heaton (1994). Spatial and temporal distribution of slip for the 1992 Landers, California, earthquake, *Bull. Seism. Soc. Am.* **84,** 668–691.

Wu, F. T., C. S. Chang, and Y. M. Wu (2004). Precisely relocated hypocenters, focal mechanisms and active orogeny in Central Taiwan, in *Aspects of the Tectonic Evolution of China, Geol. Soc. of London Special Publication 226*, 333–353.

Wu, Y. M., and L. Y. Chiao (2006). Seismic quiescence before the 1999 Chi-Chi, Taiwan Mw7.6 earthquake, *Bull. Seism. Soc. Am.* **96,** 321–327.

Wu, Y. M., R. M. Allen, and C. F. Wu (2005). Revised M_L determination for crustal earthquakes in Taiwan, *Bull. Seism. Soc. Am.* **95,** 2517–2524.

Wu, Y. M., C. H. Chang, and L. Zhao (2006). Improvement on Vp/Vs structures and earthquake location using a dense strong motion array in Taiwan, Presented at The AGU Fall Meeting, 11–15 December 2006, San Francisco, California.

Wu, Y. M., W. H. K. Lee, C. C. Chen, T. C. Shin, T. L. Teng, and Y. B. Tsai (2000). Performance of the Taiwan Rapid Earthquake Information Release System (RTD) during the 1999 Chi-Chi (Taiwan) earthquake, *Seism. Res. Lett.* **71,** 338–343.

Central Weather Bureau
Taipei 100, Taiwan
(C.-H.C.)

Department of Geosciences
National Taiwan University
Taipei 106, Taiwan
(Y.-M.W.)

Institute of Earth Sciences
Academia Sinica
Nankang, Taipei 115, Taiwan
(L.Z.)

Department of Geological Science and Environmental Studies
Binghamton University
Binghamton, New York 13902
(F.T.W.)

Manuscript received 31 August 2006.